

Article

Anomalous Hall Effect and Magneto-Optic Kerr Effect in Pt/Co/Pt Heterostructure

Yiming Sun [†], Liangwei Wu [†], Mengmeng Yang, Mengjia Xia, Wei Gao, Dongxiang Luo , Nengjie Huo ^{*} and Jingbo Li ^{*}

Institute of Semiconductors, South China Normal University, Guangzhou 510631, China; yimingsun@m.scnu.edu.cn (Y.S.); 2019022842@m.scnu.edu.cn (L.W.); mmyang@mail2.gdut.edu.cn (M.Y.); 2019022809@m.scnu.edu.cn (M.X.); gaowei317040@m.d.cnu.edu.cn (W.G.); luodx@gdut.edu.cn (D.L.)

^{*} Correspondence: njhuo@m.scnu.edu.cn (N.H.); jbli@m.scnu.edu.cn (J.L.)

[†] These authors contribute equally to this work.

Abstract: Magnetic multilayer with large perpendicular magnetic anisotropy (PMA) has attracted sustained interest owing to its importance to fundamental physics and applications. In this work, the high quality of Pt/Co/Pt heterostructures with large PMA was successfully achieved to exhibit a large anomalous Hall effect (AHE) with squared Hall loops. By calculating the proportional relationship between the longitudinal resistivity (ρ_{xx}) and the abnormal Hall coefficient (R_s), it is confirmed that the basic mechanism of AHE comes from the external skew scattering (SS) and side jump (SJ), while SS contribution, related to asymmetric scattering from impurities, is dominant in the AHE. Furthermore, the obvious magneto-optical Kerr effect (MOKE) was also observed using the polar MOKE microscopy. The obviously circular magnetic domain can form and propagate in response to the applied out-of-plane magnetic field, resulting in the magnetization reversal of the entire film. This work offers important information in terms of both AHE and MOKE in the ultrathin ferromagnetic films with perpendicular anisotropy, establishing the application foundation for the nonvolatile memories and spintronics.

Keywords: magneto-optical Kerr effect; anomalous Hall effect; perpendicular magnetic anisotropy; magnetic domain wall



Citation: Sun, Y.; Wu, L.; Yang, M.; Xia, M.; Gao, W.; Luo, D.; Huo, N.; Li, J. Anomalous Hall Effect and Magneto-Optic Kerr Effect in Pt/Co/Pt Heterostructure. *Magnetochemistry* **2022**, *8*, 56. <https://doi.org/10.3390/magnetochemistry8050056>

Academic Editors: Bo Li and Xiaoxi Li

Received: 30 March 2022

Accepted: 25 April 2022

Published: 12 May 2022

Publisher's Note: MDPI stays neutral with regard to jurisdictional claims in published maps and institutional affiliations.



Copyright: © 2022 by the authors. Licensee MDPI, Basel, Switzerland. This article is an open access article distributed under the terms and conditions of the Creative Commons Attribution (CC BY) license (<https://creativecommons.org/licenses/by/4.0/>).

1. Introduction

The anomalous Hall effect (AHE) of ferromagnets has attracted much attention owing to its potential physical principles and wide applications [1–5]. For example, Trukhanova E.L. et al. investigated the effectiveness of Ni₈₀Fe₂₀/Cu films of different thicknesses for shielding direct current and alternating current electromagnetic signals. In general, the AHE of magnetic films or oxide magnetic materials is attributed to internal and external mechanisms [6–8]. The intrinsic mechanism is not related with the impurity scattering and associated with the Berry curvature of the band structures. While the extrinsic mechanisms, including the skew scattering (SS) and side jump (SJ) contributions, are related to spin–orbit coupling-dependent scattering from impurities or interfaces. SS is derived by asymmetric electron scattering and SJ comes from the transverse displacement of the electrons wave function by impurity scattering [9,10]. So far, various kinds of strategies have been developed to modulate AHE for spintronic applications based on these mechanisms [11,12].

As the typical magnetic metal layers that have strong perpendicular magnetic anisotropy (PMA), the Co/Pt layers possess great application potential in high-density nonvolatile magnetic memories and spintronic devices [13,14]. Aboaf et al. researchers controlled different Pt components in Pt/Co alloy magnetic films to achieve different magnetization and coercivity [15]. A.V. Svalov et al. studied the influence of magnetic fields of different directions and strengths on the anomalous Hall effect in Pt/Co films with different thicknesses [16]. Through the first principal calculation and related experiments, it is confirmed

that the origin of PMA in Co/heavy metals is the hybridization 3d electron orbitals of Co and 5d electron orbitals of heavy metal in a multilayer membrane system [17–19]. In order to understand and observe the magnetization reversal process of the Pt/Co/Pt magnetic film, the magnetic domain of the film was observed using the magneto-optical Kerr microscope with the application of magnetic field outside the surface. The complete and clear magnetic domain expansion image means a large PMA in the heterostructure [13,20–23]. In this work, the mechanisms of AHE and magneto-optic Kerr effect in Pt/Co/Pt heterostructure have been studied. Our experimental results and data scaling relationships show that both SJ and SS contribute to the AHE in the Pt/Co/Pt heterostructured films and SS plays a dominant role in the AHE. In addition, the clear magnetic domain image was observed by magneto-optic Kerr microscope. The ferromagnetic heterostructures with large AHE and PMA hold great promise for magnetic sensors and nonvolatile memory.

2. Experimental Section

Magnetic thin films of Pt/Co/Pt heterostructures were prepared by magnetron sputtering with 4 mTorr pressure under Ar conditions. Lower partial pressure of nitrogen means better quality of thin film crystals [24]. The metal targets were high purity Pt (99.9%) and Co (99.9%), respectively. Firstly, 120 Å Pt layer was grown on Si/SiO₂ substrate as buffer layer and the Co layer was deposited on the Pt layer. Then, an additional 20 Å Pt layer was deposited on top of the Co layer to avoid oxidation. Figure 1 shows the X-ray diffraction (XRD) and X-ray photoelectron spectroscopy (XPS) measurements for Pt/Co/Pt heterostructures. The magnetic properties of the heterostructures at the temperatures from 100 K to 300 K are measured by PPMS. The magnetic resistance was also measured in the same temperature range by the standard four-probe technique. Magneto-optical images are observed at room temperature with a homemade magneto-optical Kerr effect (MOKE) microscope, using a LED with wavelength of 650 nm as the light source.

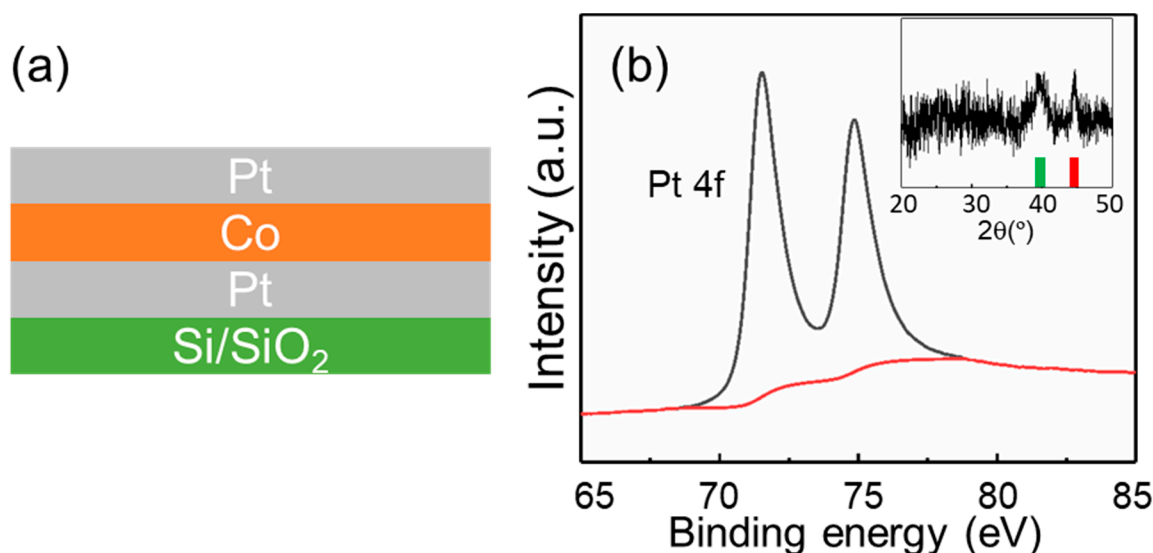


Figure 1. (a) Schematic of Pt/Co/Pt heterostructure on Si/SiO₂ substrate. (b) XPS survey spectra of the Pt in Pt/Co/Pt heterostructure. The inset is the XRD spectra of the heterostructure.

3. Results and Discussion

The architecture of the Pt/Co/Pt heterostructures is indicated in Figure 1a.

In Figure 1b, the XRD and XPS were used to further characterize the crystal quality of the magnetic film. The Pt signals with the binding energy of 72.1 eV and 75.1 eV were observed. The peak at 75.1 eV indicates that the surface of the Pt layer adsorbs the H₂O and O₂ in air [7,25]. The XRD result in the inset of Figure 1b shows the diffraction peak of

Pt is located at around 39° (Green) indicating a well (111) phase of Pt layer. The peak of 44° (Red) is corresponding to the Co (111) layer [26].

The magnetic properties of the Pt/Co/Pt film were further measured using the PPMS system. As shown in Figure 2, the film exhibits the obvious out-of-plane (OOP) magnetic hysteresis loops of Pt/Co/Pt thin films as a function of temperature, presenting squared OOP hysteresis loops indicating strong perpendicular magnetic anisotropy [27,28]. The saturation magnetization obviously decreases with decreasing temperature. On the contrary, the coercivity increases with the decrease in temperature. The large temperature dependence of the hysteresis loop is probably attributed to the 20 Å Pt with a better (111) phase, which improves the crystal and interface quality between Pt/Co. The effective anisotropy K_{eff} can be calculated by: $K_{eff} = M_s H_k / 2$, where M_s is the saturation magnetization and H_k is the anisotropy field in VSM, which measuring the area between the hard and easy axes of the magnetization curves [29,30]. When the temperature ranges from 300 to 100 K, the K_{eff} of heterostructure is calculated to be from 3.5×10^5 erg/cc to 7.5×10^5 erg/cc, showing a strong PMA and great application promise in magnetic tunnel junctions. There is a strong orbital hybridization between the Pt (heavy metals) 5d and Co 3d orbitals at the Co/Pt interface, which increases the magnetic moment of the vertical orbital in the Co layer.

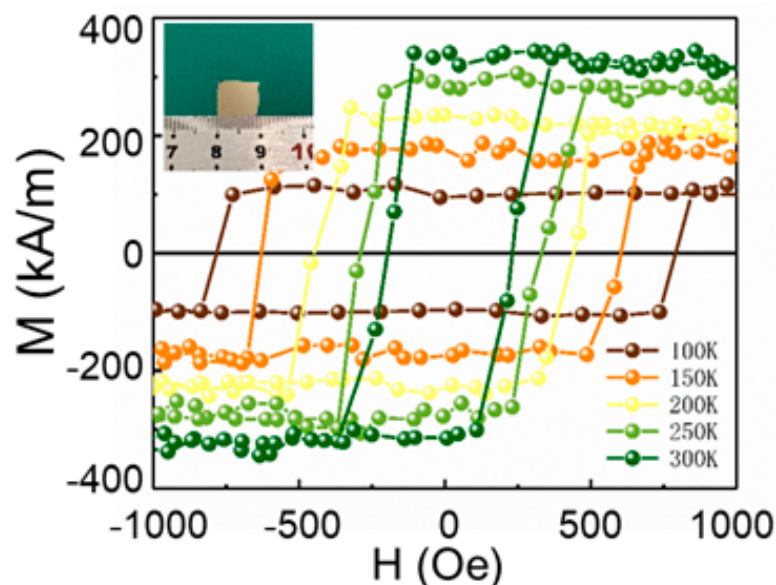


Figure 2. M-H hysteresis loops of Pt/Co/Pt heterostructure under OOP magnetic field between 100 K and 300 K. The inset is the photograph of the film.

To further study the AHE of thin films, the heterostructure devices with four electrodes Hall bar geometry are fabricated by lithography technology. Figure 3a indicates the optical microscope image of the Hall bar device. The measurement schematic is presented in Figure 3b. Direct current is applied with 100 μ A in the X-axis. The voltages in X (V_{xx}) and Y (V_{xy}) directions are measured with a magnetic field applied along the Z-direction, respectively. Figure 4a displays the dependence of the transverse Hall resistivity (ρ_{AH}) on the magnetic field at different temperatures. The M-H and ρ_{AH} -H curves show the obvious PMA in the heterostructure with the high squareness ratio of the hysteresis loop [31]. We observed the obvious anomalous Hall effect, where the ρ_{AH} exhibits squared hysteresis loop. The coercivity increases with the decrease in temperature, which is consistent with the results from the vibrating sample magnetometer measurement in Figure 2. At the field higher than coercivity, the Hall resistivity ρ_{AH} shows a linear and independence on external magnetic field because of the highly alignment of the spins. Figure 4b displays the temperature dependence of the ρ_{AH} and ρ_{xx} , respectively. ρ_{xx} is the longitudinal resistivity, which is the resistivity at the magnetic field of 0.15 T with the magnetization

reaching saturation. Both ρ_{xx} and ρ_{AH} increase significantly with increasing temperature, demonstrating the metallic behavior of the film. The metallic nature makes the interaction of spin and charge degrees of freedom form the AHE well. Figure 4c,d display the curves of $\rho_{AH}-\rho_{xx}$ and $R_s-\rho_{xx}$, respectively. There is a positive signal with Hall resistivity indicating that the Fermi level is on the side of the spin-down band, implying the majority of electron characteristics. Fermi level is on the side of the spin-down band [32]. The reason is that the heavy metal Pt layer increases the electron scattering at the Co/Pt interface, inducing the spin-orbit torque on the heterostructures [3,33–35]. To further understand the origin of the AHE, we fitted the $R_s-\rho_{xx}$ curves using a simple formula:

$$R_s = a\rho_{xx} + b\rho_{xx}^2 \quad (1)$$

where R_s is the anomalous Hall coefficient, which can be calculated by $R_s = \rho_{AH}/(M_s \times 4\pi)$, for the AHE of the heterostructure shown in Figure 4a; the fitting constants of a and b indicate the contribution of SS and SJ for AHE, respectively. From the fitting curves, the a and b are $2.09 \times 10^{-5} \text{ T}^{-1}$ and $2.45 \times 10^{-6} \mu\Omega \cdot \text{cm}/\text{T}$, respectively. The absolute magnitude of SS is an order of magnitude larger than that of the SJ, which reveals that the AHE is attributed to both SS and SJ but the contribution of SS is dominant in the AHE of the Pt/Co/Pt heterostructure.

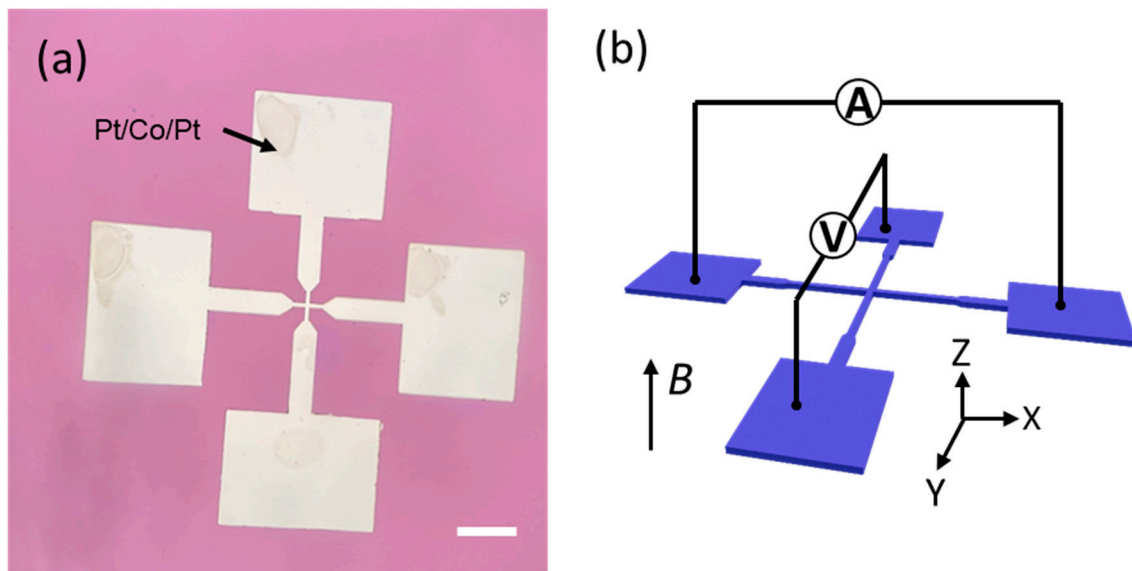


Figure 3. (a) Optical image of Pt/Co/Pt heterostructure device with Hall bar. The scale bar is 20 μm . (b) Schematic diagram of the measurement device for Hall and longitudinal resistivity.

We further used the magneto-optic Kerr microscope to characterize the magnetic domain of Pt/Co/Pt films. The polarization can be changed upon the reflection of polarized light from the surface of magnetic film, which is called magneto-optic Kerr effect (MOKE), enabling the easy observation of coercivity, magnetization reversal and domain structure. Figure 5a shows the hysteresis loops measured by MOKE. A wide-field MOKE microscope in configured polarized light is used to capture images of magnetic domains which are sensitive to out-of-plane magnetization in magnetic films. The evolution of the magnetic domain as a function of applied field by subtracting the background has been shown in Figure 5b–i. The dark and bright regions are corresponding to magnetic domains with downward and upward magnetization, respectively. Because of rectangularity of the hysteresis loop in Pt/Co/Pt film, circular magnetic domains nucleate at random positions, then diffuse and propagate in the entire film (see Supplementary Material). The magnetic domain wall is the boundary between the two regions of light and dark. The complete and clear magnetic domain expansion image because of the high-quality interface in Pt/Co/Pt can enable a stronger hybridization and a large increase in PMA.

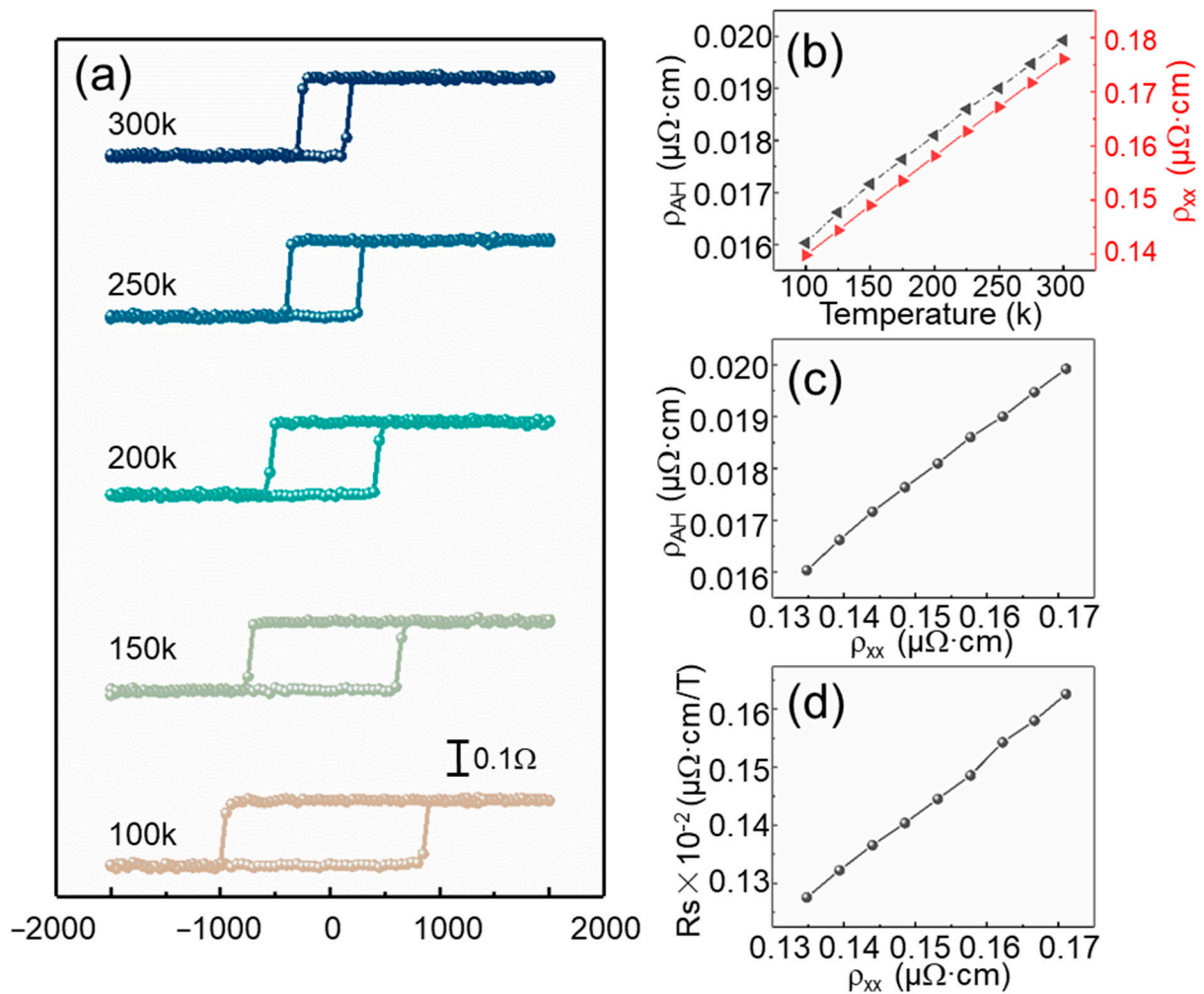


Figure 4. (a) Temperature-dependent hysteresis loop ranging from 100 K to 300 K. (b) The temperature dependence of ρ_{xx} and ρ_{AH} . (c) $\rho_{AH} - \rho_{xx}$ curves of the heterostructure. (d) The relationship curve with R_s and ρ_{xx} . The red line is the fitting curve.

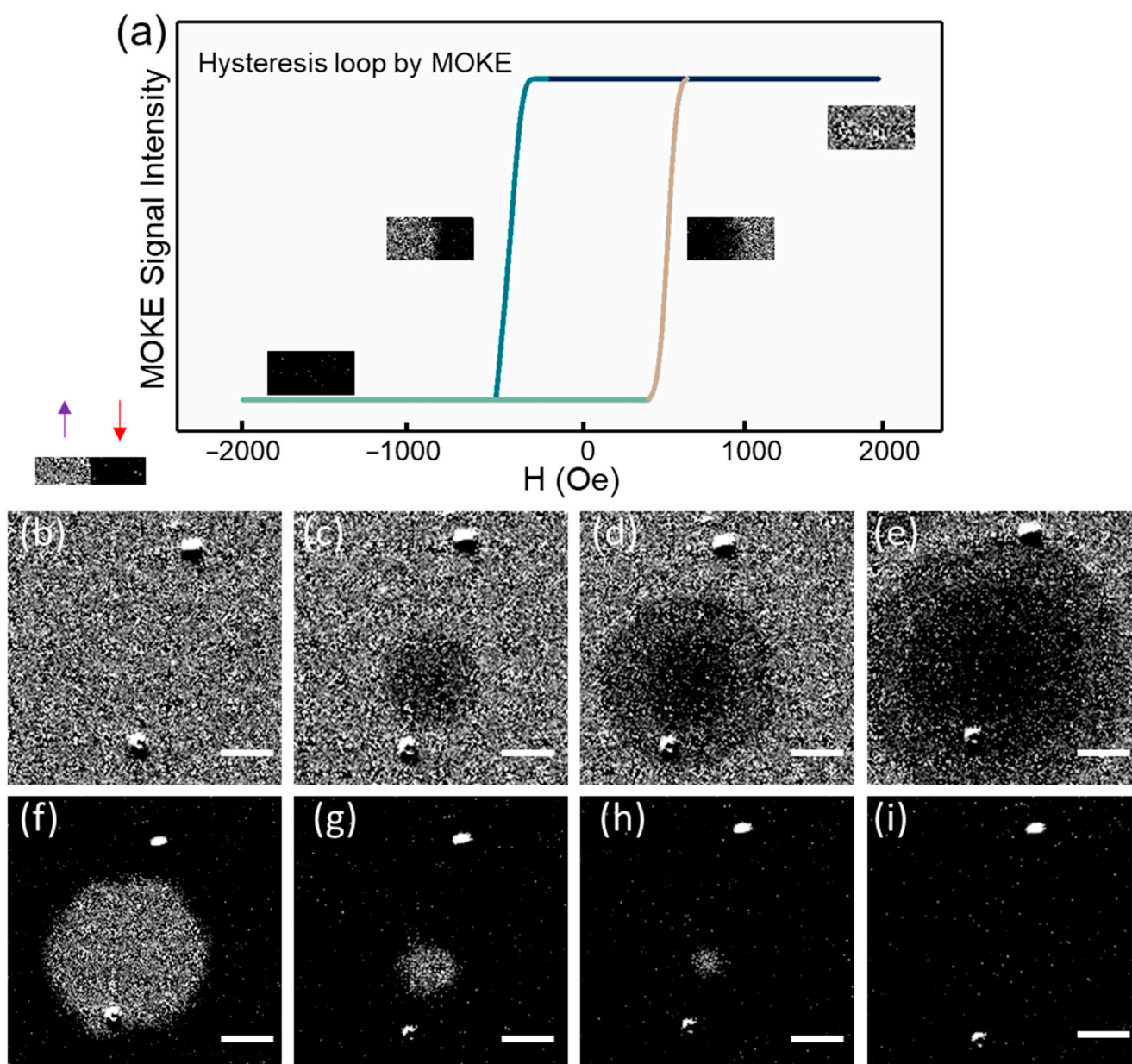


Figure 5. (a) Hysteresis loops measured by MOKE microscope. The inset shows the domains with up (white) and down (dark) magnetizations. (b–i) Image of the evolution of the magnetic domain as a function of applied field obtained after background subtraction by magneto-optic Kerr microscope. The scale bar is 5 μm .

4. Conclusions

In this work, we have successfully fabricated the Pt/Co/Pt heterostructure with superior anomalous Hall effect and magneto-optic Kerr effect. We found that the underlying mechanism of AHE is ascribed to both SS and SJ. Circular magnetic domain of the heterostructure has been clearly observed through a magneto-optic Kerr microscope. The square hysteresis loop and clear magnetic domain indicate the high quality of the ferromagnetic film with large PMA. This work offers key information for fundamental physics and potential applications of ultrathin ferromagnetic film.

Supplementary Materials: The following are available online at <https://www.mdpi.com/article/10.3390/magnetochemistry8050056/s1>, Video S1: The video for the evolution of the magnetic domain can be seen in the Supporting Information.

Author Contributions: Conceptualization, J.L. and N.H.; methodology, Y.S. and N.H.; software, L.W.; validation, L.W. and M.Y.; formal analysis, Y.S.; investigation, M.X. and W.G.; resources, D.L. and W.G.; data curation, Y.S.; writing—original draft preparation, Y.S.; writing—review and editing, N.H.; visualization, Y.S. and L.W.; supervision, N.H.; project administration, J.L. All authors have read and agreed to the published version of the manuscript.

Funding: This work was supported by China Postdoctoral Science Foundation (No.2020M672680), “The Pearl River Talent Recruitment Program” (No. 2019ZT08 × 639), the National Natural Science Foundation of China (No. 11904108, 61,874,037 and 62074060), Guangdong Basic and Applied Basic Research Foundation (Grant No. 2020B1515020032) and Natural Science Foundation of Guangdong Province (No.2018030310031).

Institutional Review Board Statement: Not applicable.

Informed Consent Statement: Not applicable.

Data Availability Statement: Not applicable.

Conflicts of Interest: The authors declare no conflict of interest.

References

1. Jiang, S.-L.; Chen, X.; Zhang, J.-Y.; Yang, G.; Teng, J.; Li, X.-J.; Cao, Y.; Zhao, Z.-D.; Yang, K.; Liu, Y.; et al. Chemically manipulated anomalous Hall effect and perpendicular magnetic anisotropy in Co/Pt multilayers. *Appl. Surf. Sci.* **2014**, *320*, 263–266. [[CrossRef](#)]
2. Zhang, Q.; Zheng, D.; Wen, Y.; Zhao, Y.; Mi, W.; Manchon, A.; Boulle, O.; Zhang, X. Effect of surface roughness on the anomalous Hall effect in Fe thin films. *Phys. Rev. B* **2020**, *101*, 134412. [[CrossRef](#)]
3. Ma, L.; Fu, H.R.; Tang, M.; Qiu, X.P.; Shi, Z.; You, C.Y.; Tian, N.; Zheng, J.-G. Static and dynamic origins of interfacial anomalous Hall effect in W/YIG heterostructures. *Appl. Phys. Lett.* **2020**, *117*, 122405. [[CrossRef](#)]
4. Bai, H.; Zhu, W.; You, Y.; Chen, X.; Zhou, X.; Pan, F.; Song, C. Size-dependent anomalous Hall effect in noncollinear antiferromagnetic Mn₃Sn films. *Appl. Phys. Lett.* **2020**, *117*, 052404. [[CrossRef](#)]
5. Trukhanov, A.V.; Grabchikov, S.S.; Solobai, A.A.; Tishkevich, D.I.; Trukhanov, S.V.; Trukhanova, E.L. AC and DC-shielding properties for the Ni₈₀Fe₂₀/Cu film structures. *J. Magn. Magn. Mater.* **2017**, *443*, 142–148. [[CrossRef](#)]
6. Liu, Y.; Liu, Y.; Cai, K.; Ren, L.; Zheng, Y.; Yang, H.; Teo, K.L. Anomalous Hall Effect of Fe₂CoSi/Pt Multilayers With Large Perpendicular Magnetic Anisotropy. *IEEE Trans. Magn.* **2018**, *54*, 2600104. [[CrossRef](#)]
7. Zhang, F.; Liu, Z.; Wen, F.; Liu, Q.; Li, X.; Ming, X. Magnetoresistance and Anomalous Hall Effect with Pt Spacer Thickness in the Spin-Valve Co/Pt/[Co/Pt]₂ Multilayers. *J. Supercond. Nov. Magn.* **2016**, *30*, 533–538. [[CrossRef](#)]
8. Turchenko, V.A.; Trukhanov, S.V.; Kostishin, V.G.E.; Damay, F.; Porcher, F.; Klygach, D.S.; Vakhitov, M.G.E.; Matzui, L.Y.E.; Yakovenko, O.S.; Bozzo, B.; et al. Impact of In³⁺ cations on structure and electromagnetic state of M–type hexaferrites. *J. Energy Chem.* **2022**, *69*, 667–676. [[CrossRef](#)]
9. Dugaev, V.K.; Bruno, P.; Taillefumier, M.; Canals, B.; Lacroix, C. Anomalous Hall effect in a two-dimensional electron gas with spin-orbit interaction. *Phys. Rev. B* **2005**, *71*, 224423. [[CrossRef](#)]
10. Yao, Y.; Kleinman, L.; MacDonald, A.H.; Sinova, J.; Jungwirth, T.; Wang, D.S.; Wang, E.; Niu, Q. First principles calculation of anomalous Hall conductivity in ferromagnetic bcc Fe. *Phys. Rev. Lett.* **2004**, *92*, 037204. [[CrossRef](#)]
11. Chen, T.-Y.; Liao, W.-B.; Chen, T.-Y.; Tsai, T.-Y.; Peng, C.-W.; Pai, C.-F. Current-induced spin–orbit torque efficiencies in W/Pt/Co/Pt heterostructures. *Appl. Phys. Lett.* **2020**, *116*, 072405. [[CrossRef](#)]
12. Koyama, T.; Ieda, J.; Chiba, D. Electric field effect on the magnetic domain wall creep velocity in Pt/Co/Pd structures with different Co thicknesses. *Appl. Phys. Lett.* **2020**, *116*, 092405. [[CrossRef](#)]
13. Wang, X.; Wei, Y.; He, K.; Liu, Y.; Huang, Y.; Liu, Q.; Wang, J.; Han, G. Effect of the repeat number and Co layer thickness on the magnetization reversal process in [Pt/Co(x)]_N multilayers. *J. Phys. D Appl. Phys.* **2020**, *53*, 215001. [[CrossRef](#)]
14. Kawaguchi, M.; Towa, D.; Lau, Y.-C.; Takahashi, S.; Hayashi, M. Anomalous spin Hall magnetoresistance in Pt/Co bilayers. *Appl. Phys. Lett.* **2018**, *112*, 202405. [[CrossRef](#)]
15. Aboaf, J.A.; Herd, S.R.; Klockholm, A.E. Magnetic Properties and Structure of CobaltPlatinum Thin Films. *IEEE Trans. Magn.* **1983**, *MAG-1*, 1514–1519. [[CrossRef](#)]
16. Sorokin, A.N.; Svalov, A.V. Magnetic and galvanomagnetic properties of CoPt films. *J. Magn. Magn. Mater.* **1995**, *146*, 214–216. [[CrossRef](#)]
17. Hashimoto, S.; Ochiai, Y.; Aso, K. Perpendicular magnetic anisotropy and magnetostriction of sputtered Co/Pd and Co/Pt multilayered films. *J. Appl. Phys.* **1989**, *66*, 4909–4916. [[CrossRef](#)]
18. Carcia, P.F. Perpendicular magnetic anisotropy in Pd/Co and Pt/Co thin-film layered structures. *J. Appl. Phys.* **1988**, *63*, 5066–5073. [[CrossRef](#)]
19. Kim, D.; Hong, J. Perpendicular magnetic anisotropy of ultrathin FeCo alloy films on Pd(001) surface: First principles study. *J. Magn. Magn. Mater.* **2009**, *321*, 1821–1827. [[CrossRef](#)]

20. Khan, R.A.; Nembach, H.T.; Ali, M.; Shaw, J.M.; Marrows, C.H.; Moore, T.A. Magnetic domain texture and the Dzyaloshinskii-Moriya interaction in Pt/Co/IrMn and Pt/Co/FeMn thin films with perpendicular exchange bias. *Phys. Rev. B* **2018**, *98*, 064413. [[CrossRef](#)]
21. Wang, X.; Liu, Y.; Wei, Y.; He, K.; Huang, Y.; Wang, J.; Liu, Q.; Han, G. Magnetic properties and magnetization reversal process in (Pt/CoFe/MgO)₁₀ multilayers at low temperature. *J. Magn. Magn. Mater.* **2020**, *499*, 166318. [[CrossRef](#)]
22. Domenichini, P.; Quinteros, C.P.; Granada, M.; Collin, S.; George, J.M.; Curiale, J.; Bustingorry, S.; Capeluto, M.G.; Pasquini, G. Transient magnetic-domain-wall ac dynamics by means of magneto-optical Kerr effect microscopy. *Phys. Rev. B* **2019**, *99*, 214401. [[CrossRef](#)]
23. Yamamoto, K.; Moussaoui, S.E.; Hirata, Y.; Yamamoto, S.; Kubota, Y.; Owada, S.; Yabashi, M.; Seki, T.; Takashi, K.; Matsuda, I.; et al. Element-selectively tracking ultrafast demagnetization process in Co/Pt multilayer thin films by the resonant magneto-optical Kerr effect. *Appl. Phys. Lett.* **2020**, *116*, 172406. [[CrossRef](#)]
24. Svalov, A.V.; Aseguinolaza, I.R.; Garcia-Arribas, A.; Orue, I.; Barandiaran, J.M.; Alonso, J.; Fernández-Gubieda, M.L.; Kurlyandskaya, G.V. Structure and Magnetic Properties of Thin Permalloy Films Near the “Transcritical” State. *IEEE Trans. Magn.* **2010**, *46*, 333–336. [[CrossRef](#)]
25. Zubar, T.I.; Fedosyuk, V.M.; Trukhanov, S.V.; Tishkevich, D.I.; Michels, D.; Lyakhov, D.; Trukhanov, A.V. Method of surface energy investigation by lateral AFM: Application to control growth mechanism of nanostructured NiFe films. *Sci. Rep.* **2020**, *10*, 14411. [[CrossRef](#)]
26. Subhi, A.A.; Sbiaa, R. Control of magnetization reversal and domain structure in (Co/Ni) multilayers. *J. Magn. Magn. Mater.* **2019**, *489*, 165460. [[CrossRef](#)]
27. Wang, X.; Zhu, Z.; Ma, L.; Feng, H.; Xie, H.; Wang, J.; Liu, Q.; Han, G. Influence of Deposition Cycle and Magnetic Annealing on High-Frequency Magnetic Properties of the [Co₉₀Fe₁₀/Ta]_n Multilayer Thin Films. *IEEE Trans. Magn.* **2018**, *54*, 2800607. [[CrossRef](#)]
28. Sharko, S.A.; Serokurova, A.I.; Novitskii, N.N.; Ketsko, V.A.; Smirnova, M.N.; Almuqrin, A.H.; Sayyed, M.I.; Trukhanov, S.V.; Trukhanov, A.V. A New Approach to the Formation of Nanosized Gold and Beryllium Films by Ion-Beam Sputtering Deposition. *Nanomaterials* **2022**, *12*, 470. [[CrossRef](#)]
29. Wu, Y.; Zhang, J.; Wang, Z.C.; Wang, J.; Xu, X.G.; Miao, J.; Zhang, J.X.; Jiang, Y. Perpendicular magnetic anisotropy and thermal stability in Co₂FeAl_{0.5}Si_{0.5}/Pt multilayers. *Appl. Phys. A* **2014**, *117*, 773–779. [[CrossRef](#)]
30. Wu, Y.; Xu, X.G.; Miao, J.; Jiang, Y. Perpendicular Magnetic Anisotropy in Co-Based Full Heusler Alloy Thin Films. *Spin* **2016**, *5*, 1540012. [[CrossRef](#)]
31. Jagla, E.A. Hysteresis loops of magnetic thin films with perpendicular anisotropy. *Phys. Rev. B* **2005**, *72*, 094406. [[CrossRef](#)]
32. Meng, K.K.; Miao, J.; Xu, X.G.; Xiao, J.X.; Zhao, J.H.; Jiang, Y. Anomalous Hall effect in Mn_{1.5}Ga/Ta and Mn_{1.5}Ga/Pt bilayers: Modification from spin-orbit coupling of heavy metals. *Phys. Rev. B* **2016**, *93*, 060406. [[CrossRef](#)]
33. Wu, Y.; Zhang, J.; Xiong, Q.; Gao, S.; Xu, X.; Miao, J.; He, Z.; Jiang, Y. The Anomalous Hall Effect of Co₂FeAl_{0.5}Si_{0.5}/Pt Multilayers with Perpendicular Magnetic Anisotropy. *Appl. Phys. Express* **2013**, *6*, 113003. [[CrossRef](#)]
34. Loong, L.M.; Deorani, P.; Qiu, X.; Yang, H. Investigating and engineering spin-orbit torques in heavy metal/Co₂FeAl_{0.5}Si_{0.5}/MgO thin film structures. *Appl. Phys. Lett.* **2015**, *107*, 022405. [[CrossRef](#)]
35. Trukhanov, S.V.; Lobanovski, L.S.; Bushinsky, M.V.; Khomchenko, V.A.; Pushkarev, N.V.; Troyanchuk, I.O.; Maignan, A.; Flahaut, D.; Szymczak, H.; Szymczak, R. Influence of oxygen vacancies on the magnetic and electrical properties of La_{1-x}Sr_xMnO_{3-x/2} manganites. *Eur. Phys. J. B* **2004**, *42*, 51–61. [[CrossRef](#)]